Development 134, 2227-2236 (2007) doi:10.1242/dev.004952

Actin-dependent cytoplasmic streaming in *C. elegans* oogenesis

Uta Wolke[1,3], Erin A. Jezuit[1,2] and James R. Priess[1,2,3,*]

Oocytes in the *C. elegans* gonad enlarge rapidly. During the stage of enlargement, they are transcriptionally quiescent, and it is not understood how they acquire large quantities of materials such as mRNA and protein. Enlarging oocytes are connected via cytoplasmic bridges to a large, younger population of transcriptionally active germ cells at various stages of mitosis and meiosis. We show here that there is a general streaming of gonad cytoplasm towards and into the enlarging oocytes, originating primarily from pachytene-stage germ cells. Because previous studies suggested that most or all of the pachytene germ cells have the potential to differentiate into oocytes, the pachytene cells appear to function transiently as nurse cells. Somatic gonadal cells that surround the germ cells do not appear essential for streaming. Instead, materials appear to be pulled into oocytes by forces generated either in, or adjacent to, the enlarging oocytes themselves. Streaming appears to be driven by the actomyosin cytoskeleton, although we show that populations of both microfilaments and microtubules are oriented in the direction of flow. Our study shows that oocyte enlargement in *C. elegans* differs significantly from that in *Drosophila*, where a small number of specialized nurse cells expel their contents into the enlarging oocyte.

KEY WORDS: Actin, Cytoskeleton, *C. elegans*, Cytoplasmic streaming, Oogenesis

INTRODUCTION

A fully grown *C. elegans* oocyte is a large cell with a volume equivalent to the 558 cells it will generate during embryogenesis. Oocytes are ovulated every ~23 minutes, a rate of biosynthesis that is equivalent to the entire gonad doubling in size every 6.5 hours (Hirsh et al., 1976; McCarter et al., 1999). Most of the growth of the oocyte occurs during stages when its nucleus appears to be transcriptionally quiescent, raising the issue of where oocyte materials originate (Starck, 1977). In many animals with large oocytes, much of the oocyte volume consists of yolk lipoproteins. The yolk lipoproteins are typically secreted by non-gonadal tissues, such as the liver in vertebrates or the fat body in *Drosophila*, and then taken up into oocytes by endocytosis (Valle, 1993). Similarly, *C. elegans* oocytes use receptor-mediated endocytosis to take up yolk proteins that are secreted into the body cavity by intestinal cells (Grant and Hirsh, 1999; Kimble and Sharrock, 1983). However, fully grown *C. elegans* oocytes that lack the yolk receptor RME-2 are only slightly smaller than wild-type oocytes, indicating that yolk does not constitute most of the oocyte volume (Grant and Hirsh, 1999).

C. elegans oocytes are incompletely cellularized until late stages of oocyte development; the growing oocytes are linked through cytoplasmic bridges to a shared anucleate region called the gonad core (see Fig. 1A). The core extends through most of the adult gonad, interconnecting hundreds of germ cells at various stages of mitosis, meiosis and oogenesis. Similar cytoplasmic bridges link small groups of germ cells, called cysts, in *Drosophila*, *Xenopus* and mice (Pepling et al., 1999). Although the bridges may have different functions in male and female germlines, or at different times in germline development, at least one important function of the bridges during *Drosophila* oocyte development is in cytoplasmic transport (reviewed by Cooley and Theurkauf, 1994; Mahajan-Miklos and Cooley, 1994). Only one cell in the 16-cell *Drosophila* cyst becomes an oocyte; the other 15 cells become highly polyploid 'nurse' cells that contribute protein and RNA to the oocyte, and eventually die by apoptosis (Cavaliere et al., 1998).

C. elegans gonads do not contain morphologically distinct nurse cells, and none of the germline nuclei appear to be highly polyploid when stained for DNA (Hirsh et al., 1976) (our unpublished data). Prior to oogenesis, most germ cells appear to be highly active transcriptionally, producing RNA that accumulates in the gonad core (Gibert et al., 1984; Starck, 1977). As the transcriptionally quiescent oocytes enlarge, they presumably incorporate core cytoplasm that they, or other germ cells, synthesized during earlier developmental stages and deposited in the core. Thus, most germ cells could function transiently as nurse cells before becoming gametes. It has been estimated that about half of all *C. elegans* germ cells die by apoptosis around the end of the pachytene stage (Gumienny et al., 1999); if these germ cells contribute material to the core before dying, they might function solely as nurse cells. However, all *C. elegans* germ cells appear to have the potential to differentiate into functional gametes if the apoptotic pathway is blocked (Gumienny et al., 1999).

The mechanism through which core cytoplasm is incorporated into *C. elegans* oocytes is not understood. The oocyte plasma membranes could simply extend across the core, slicing off a section of adjacent cytoplasm (Hirsh et al., 1976). For example, in the transition from syncytial blastoderm to cellular blastoderm in *Drosophila* embryos, cytoplasm is engulfed as the plasma membrane invaginates between nuclei and progressively furrows into the egg (Foe and Alberts, 1983). Alternatively, core cytoplasm could be transported into *C. elegans* oocytes, analogous to the movement of nurse cell cytoplasm into *Drosophila* oocytes. In the early stages of *Drosophila* oogenesis, there is a steady movement of nurse cell cytoplasm into the enlarging oocyte through cytoplasmic bridges, here termed ring canals (Mahajan-Miklos and Cooley, 1994). Inhibitor studies have suggested that movement of particles

[1]Division of Basic Sciences, Fred Hutchinson Cancer Research Center, Seattle, WA 98109, USA. [2]Molecular and Cellular Biology Program and Department of Biology, University of Washington, Seattle, WA 98195, USA. [3]Howard Hughes Medical Institute, Seattle, WA 98109, USA.

*Author for correspondence (e-mail: jpriess@fred.fhcrc.org)

Accepted 6 April 2007

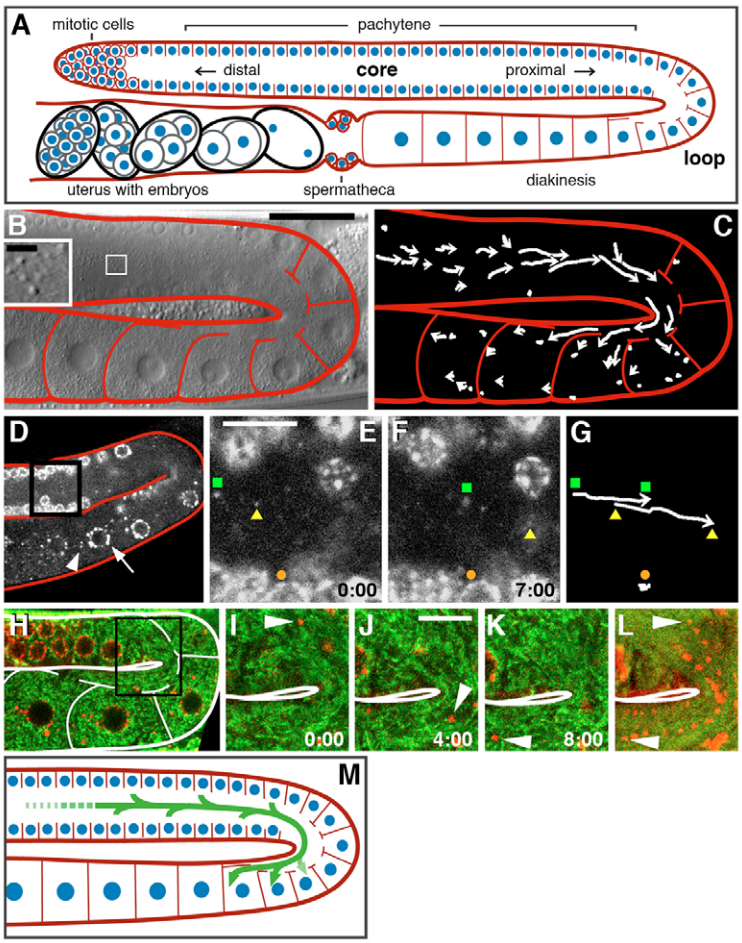

Fig. 1. Proximal streaming in the wild-type *C. elegans* gonad. (**A**) Diagram of one arm of an adult hermaphrodite gonad. Plasma membranes, red; nuclei, blue. Somatic sheath cells enclose most of the gonad, but are not shown for simplicity. (**B**) Single image from time-lapse movie. DIC particles are shown at high magnification in inset. (**C**) 2-minute particle tracks. Arrows indicate final positions of particles and dots indicate stationary particles. Most particles ceased movement in cellularized oocytes; the small arrows shown result primarily from a shift in oocyte position. (**D-G**) Movement of PGL-1::GFP particles. (D) Low magnification view of gonad indicating perinuclear P granules (arrow) and detached, cytoplasmic P granules (arrowhead). (E-G) Time-lapse series of boxed region in D. Particles tracked are a perinuclear P granule (orange circle) and cytoplasmic PGL-1::GFP particles (green square and yellow triangle). Movements are summarized in G. (**H**) Low magnification view of gonad showing PGL-1:: mRFP-1 (red) and mitochondria (green). For movements of mitochondria see Movie 1 in the supplementary material. (**I-K**) Time-lapse images of a single PGL-1::mRFP-1 particle (arrowhead). Time is shown in minutes. (**L**) Composite of particle positions at 15 time points in 30-second intervals. (**M**) Diagram of bulk particle movement (green). Scale bars: 30 μm in B; 3 μm in B inset; 10 μm in E,J.

such as mitochondria and lipid droplets through the ring canals is dependent on microfilaments, but not microtubules, although large numbers of microtubules are present in the ring canals (Bohrmann and Biber, 1994; Theurkauf et al., 1992). However, a GFP-tagged Exuperantia fusion protein appears to move through the ring canals independently of microfilaments (Theurkauf and Hazelrigg, 1998). Late in oogenesis, the nurse cells undergo apoptosis and expel their remaining contents into the oocyte through a process called dumping. Dumping is thought to be mediated by the contraction of the actin/myosin-rich cortex of the nurse cells (reviewed by Robinson and Cooley, 1997).

In this paper, we demonstrate that there is bulk streaming of cytoplasmic materials in the core of the *C. elegans* gonad, moving material into enlarging oocytes. We show that contractions of the somatic sheath cells surrounding the gonad are not essential for streaming. We demonstrate that long microtubules are present in the cytoplasmic bridges between the growing oocytes and the core cytoplasm, but that microtubule function does not appear essential for bulk streaming into oocytes. Instead, this streaming appears to involve actin- and myosin-dependent forces generated either in the enlarging oocytes themselves, or immediately adjacent to the oocytes.

MATERIALS AND METHODS

C. elegans maintenance

Nematodes were cultured and manipulated genetically as described by Brenner (Brenner, 1974). Unless otherwise indicated, experiments were performed on the wild-type N2 strain (var. Bristol), maintained at room temperature (22-23°C) and analyzed as soon as they were fully gravid (12-24 hours after last molt). The following strains and alleles were used: *fem-1(hc17ts)*, *fem-3(q20gf)* (Barton et al., 1987), *fog-1(q241)* (Barton and Kimble, 1990), *VIT-2::GFP* (*YP-170::GFP*; strain DH1033) and *rme-2(b1008)* (Grant and Hirsh, 1999). *fem-1(hc17ts)* worms were shifted to the restrictive temperature (25°C) at the L1 stage. *fem-3(q20gf)* hermaphrodites were raised at semi-permissive temperature (15°C), and analyzed 1 day after the final molt. *fog-1(q241)/hT2::pharyngeal GFP* was kindly provided by Tim Schedl (Washington University School of Medicine, St Louis, MO). Homozygous *fog-1(q241)* 'males' (XO animals with feminized germline that produce oocytes) were grown at 17°C and analyzed when they produced oocytes.

Plasmid construction and generation of transgenic strains

Standard techniques were used to amplify and manipulate DNA. The Advantage High Fidelity PCR Kit (Clontech) was used for all PCR procedures. pUW005 (*nmy-2::PGL-1::GFP; unc-119*): the *nmy-2* coding region present in the *nmy-2::GFP; unc-119* plasmid (Nance et al., 2003) was replaced with PCR-amplified genomic *pgl-1* coding sequence. pUW024 (*nmy-2::PGL-1::mRFP-1; unc-119*): the *gfp* coding sequence in pUW005 was replaced with *mRFP-1* amplified from the plasmid [*mRFP-1in pRSET*$_B$] (Campbell et al., 2002). Transgenic strains expressing these plasmids were obtained by microparticle bombardment of *unc-119* worms (Praitis et al., 2001).

Time-lapse imaging, image analysis and oocyte volume measurements

Individual adult worms were anaesthetized by incubation in M9 buffer (Brenner, 1974) containing 0.01% levamisole (Sigma) for about 5 minutes. Gonads were imaged within intact worms, unless stated otherwise. Worms were transferred onto agarose pads (4% agarose in M9), a coverslip was added and the resulting chamber sealed with petroleum jelly.

Differential interference contrast (DIC) 4D time-lapse movies were acquired as described (Thomas et al., 1996) using 4D Grabber (v. 1.32) software (C. Thomas, Integrated Microscopy Resource, University of Wisconsin, Madison, WI). Frames were recorded at 15-second intervals. Movies were analyzed using ImageJ (v. 1.33) software (http://rsb.info.nih.gov/ij/). Particle tracks were generated using the ImageJ 'manual tracking' plug-in. Individual particles were tracked for 2-minute intervals, unless indicated otherwise. Particle speeds were then calculated for each time point and averaged over the 2-minute time interval using Microsoft Excel (v. 11.1.1).

Area and length measurements of oocytes were performed with ImageJ (v. 1.33) software (http://rsb.info.nih.gov/ij/) and Microsoft Excel (v. 11.1.1). Oocyte volumes before and after influx were 5682±1000 and 13729±3000 μm^3, respectively, corresponding to a 2.4-fold increase in size (n=19 oocytes; six movies). Fully mature oocytes that have taken up yolk are 21700±4000 μm^3 (n=8 oocytes), suggesting that 37% of the final volume originates from streaming. Flux measurements generate a similar estimate of 29%: oocytes are ovulated every 23 minutes (McCarter et al., 1999) and the cytoplasmic flux through the late pachytene zone is [core diameter (7.6 μm)/2]$^2 \times \pi \times$ flow velocity (6 μm/minute at 22°C)=272 μm^3/minute (n=6 animals).

Confocal time-lapse movies were obtained using a Leica TCS SP microscope and Leica Confocal software, and a Zeiss LSM 510 and Zeiss software. We used argon (488 nm) and helium/neon (543 nm) lasers. Laser powers at the sample were in the range 0.01-0.07 mW (exception: Movie 1, 0.5 mW for red channel). Pinhole size was between 0.9 and 3.4 Airy units. To label mitochondria, worms were fed overnight on bacterial lawns soaked with 1 ml of $DiOC_6(3)$ solution (2 μg/ml).

Imaging of extruded gonads and drug treatments

Worms were picked onto a coverslip, into a drop of freshly made embryonic culture medium [ECM; modified from Park and Priess (Park and Priess, 2003): 84% L-15 (Leibovitz L15 with L-glutamine, without Phenol Red; Gibco), 9.3% fetal calf serum (Gibco), 4.7% sucrose, 0.01% levamisole, 2 mM EGTA]. Worms were cut behind the pharynx to extrude gonads. Many gonads appear damaged after extrusion and do not display streaming (data not shown); these gonads were removed. For drug treatments, ECM containing latrunculin A (Sigma), ML-7 (Calbiochem) or DMSO (for controls) was then added. The coverslip was inverted onto an agarose pad (0.8% agarose in water, soaked in ECM and inhibitor drugs). The pad was surrounded by petroleum jelly spacers and, after applying gentle pressure to the coverslip, the chamber was sealed as above. DIC time-lapse movies (see above) were recorded starting no later than 10 minutes after extrusion. Some movies, of both experimental and control gonads, were discarded based on abnormal morphology such as loops and constrictions that formed during the movie.

Visualization of microtubules by immunofluorescence

Cut worms with extruded gonads were fixed in 2% paraformaldehyde in 75 mM PIPES pH 7.0, 10 mM EGTA, 10 mM $MgCl_2$ for 15 minutes, then rinsed once with PBS and three times with 75 mM PIPES pH 7.0. Gonads were dissected free from body tissues and transferred by mouth pipette to a Teflon-coated slide (Erie Scientific) treated with 0.1% polylysine (Sigma). Gonads were gently compressed by drawing across an eyelash glued to a toothpick. Nearly all of the fluid surrounding the gonads was removed by mouth pipette, and the slides immersed in –20°C methanol for 10 minutes. Slides were rinsed in PBS containing 0.1% Tween 20 (Sigma) and immunostained with anti-tubulin antibody YL1/2 (Boehringer Mannheim); imaging was performed with a Leica TCS SP scanning confocal microscope.

Phalloidin staining

In method I, Gonads were dissected in culture buffer (1.6% sucrose, 73 mM HEPES pH 6.9, 40 mM NaCl, 5 mM KCl, 2 mM $MgCl_2$, 10 mM EGTA) containing 0.5 mM levamisole, then fixed in 3% formaldehyde, 73 mM HEPES (pH 6.9), 40 mM NaCl, 5 mM KCl, 2 mM $MgCl_2$, 10 mM EGTA for 5-10 minutes. Gonads were rinsed briefly in PBS, permeabilized in 0.025% Triton X-100 in PBS for 5 minutes, then rinsed in PBS and stained with Alexa Fluor 488 phalloidin (Invitrogen) for 20 minutes. Fixation method II is identical to method I except that 15 mM sodium azide (Sigma) was substituted for levamisole in the culture buffer. In a typical experiment, no more than 1.5 minutes elapsed between placing the worms in the buffer, dissecting and adding fixative. Alternatively, worms could be dissected in buffer without azide, and then sodium azide was added for 20 seconds before fixation. Live gonads expressing the actin-binding protein GFP-moesin (Motegi et al., 2006) that were exposed to sodium azide at this concentration showed no evidence of de novo formation or aggregation of actin filaments, suggesting that the azide treatment stabilized an existing actin population.

RNA interference

RNAi against tubulin genes: wild-type L4-stage worms were fed with *tba-2*, *tbb-1* and *tbb-2* feeding strains from the Ahringer laboratory RNAi feeding library at 25°C (Kamath and Ahringer, 2003). As a control, we used an empty-vector feeding strain.

Dynein heavy chain (*dhc-1*) RNAi: a 603 bp fragment of the *dhc-1* gene was amplified from worm genomic DNA (N2 strain) using T7-tagged primers 5′-ATCGATAATACGACTCACTATAGGGTCTTCATCCGCC-CTCGT-3′ and 5′-ATCGATAATACGACTCACTATAGGGGCTGAT-GGACGCATCTGA-3′. Double-stranded RNA (dsRNA) was then synthesized using standard techniques and injected into adult wild-type gonads (Fire et al., 1998). Worms were analyzed 24-30 hours after injection.

Additional microtubule associated protein genes depleted by RNAi (soaking or injection): F42A6.3, C36A4.5, F32A7.5, *lgg-1*, *lgg-2*, F54A3.1, T08D2.8, F53F4.3, *dnc-1*, Y79H2A.11, W0761.5, *dhc-1*, *che-3*, B0365.7, W05B2.4, C17H12.1, *dli-1*, *dlc-1*, Y10G11A.2, Y10G11A.3, M18.2, F41G4.1, F13G3.4, T05C12.5, D1009.5.

Injection of mineral oil drops and microspheres

Young adult worms were injected with drops of mineral oil (heavy white oil, Sigma) into one or both gonad arms, using techniques as described (Mello et al., 1991) (http://www.wormbook.org/). The worms spent a maximum of 5 minutes on the injection pads, and were then transferred in M9 buffer to bacterial lawns. Only worms that moved normally were analyzed further. Time-lapse movies (see above) were started 20 minutes after the injection was completed.

Fluorescent polystyrene microspheres [FluoSpheres, carboxylate-modified microspheres, 0.2 microns, red fluorescent (580/605 nm), Molecular Probes] for injection were washed four times in water, incubated in 1% bovine serum albumin in 50 mM phosphate buffer (pH 7.4) for 1 hour, washed twice and then resuspended in phosphate buffer (pH 7.4).

RESULTS

Background: gonad morphology

Each of the two arms of the adult hermaphrodite gonad is a simple tube with a U-shaped bend (the loop region, see Fig. 1A); for a detailed description of gonad morphology and development see Schedl (Schedl, 1997) and Worm Book online (http://www.wormbook.org/). The gonad is composed almost entirely of germ cells; a few somatic cells called sheath cells partially surround the gonad. Throughout most of the gonad, germ nuclei are located at the periphery of the gonad, encircling a large anucleate zone called the core of the gonad (or rachis). The plasma membrane around each germ nucleus is incomplete, creating an intercellular bridge with the core. We refer to these circular openings between the germ cells and the core as ring channels. Although most *C. elegans* germ nuclei are syncytial, it is conventional to refer to a nucleus, the associated cytoplasm and membranes as a 'germ cell'. Mitosis in the germline occurs at the distal end of each gonad arm (away from the uterus and vulva), eventually producing about 1000 germ cells that enter successive stages of meiosis as they move proximally (towards the uterus). Most of the distal half of the gonad consists of nuclei at the pachytene stage of meiotic prophase I; for convenience, we subdivide this region into equally sized early, mid, and late pachytene regions. In fourth-larval-stage hermaphrodites, the first set of about 150 germ cells differentiate as sperm in the proximal

Table 1. DIC particle speeds in young adult wild-type worms

Area of the gonad	Speed*	$n^{\dagger}$
Distal tip	0.1±0.6	3; 20
Early pachytene	0.3±1.2	3; 29
Mid pachytene	1.4±1.2	6; 52
Late pachytene	6.0±2.1	3; 29
Proximal of the loop	7.0±1.9	3; 25
Particles entering oocytes	8.0±2.3	3; 25
Right after entering oocytes	2.7±1.2	3; 33

Particle speeds were measured in young adult wild-type worms (12-24 hours after last molt) as described in Materials and methods.
*Average speed in μm/minute±s.d.
†Number of worms analyzed; total number of particles analyzed.

region of the gonad; subsequent adult germ cells differentiate as oocytes. The oocytes begin to enlarge in the loop area, and finally sever their connection to the core (cellularization) after leaving the loop. Oocyte meiotic maturation is signaled by extracellular major sperm protein (MSP) from sperm in the spermatheca; mature oocytes are ovulated into the spermatheca and fertilized (for a review, see Greenstein, 2005).

Particle movement in the gonad core

To determine the source of cytoplasmic materials incorporated into enlarging oocytes, we generated time-lapse movies of gonads within anaesthetized wild-type adult hermaphrodites. Cytoplasmic particles of various sizes are visible by differential interference contrast (DIC) microscopy throughout the gonad core (Fig. 1B, inset) and in enlarging oocytes. The movements of individual particles could be traced in time-lapse recordings for several minutes. We found that the membranes of an enlarging oocyte did not simply spread across and engulf stationary particles in the adjacent core cytoplasm. Instead, particles in the core moved towards and into the enlarging oocytes concomitant with an increase in oocyte size (Fig. 1B,C). Particles in the distal third of the gonad (mitotic to early pachytene zones) appeared stationary or exhibited only brief, apparently random movements (Table 1). By contrast, large numbers of moving particles were present in the mid-to-late pachytene zones (Table 1). A few particles in the pachytene zone moved radially, from the gonad periphery towards the central midline of the core (Fig. 1C). However, the vast majority of particles moved parallel to the long axis of the gonad, in a distal to proximal direction. The rate of particle movement gradually increased from the pachytene zone to the area of the enlarging oocytes (Table 1), with 1-3 oocytes close to the loop receiving most of the particles at any given time. Upon entering an enlarging oocyte, particle movement diminished and ceased rapidly; there was, for example, no general ‘swirling’ of oocyte contents (Fig. 1C).

To examine the behavior of specific cytoplasmic components, we first labeled mitochondria with the vital dye $DiOC_6(3)$ (Korchak et al., 1982). We found that there was a general, proximal flow of mitochondria along the core (see Movie 1 in the supplementary material), similar to the movement of the DIC particles. In addition, we observed several examples of mitochondria that first moved radially away from positions near pachytene nuclei, and then moved proximally (data not shown). We next examined the germ cell-specific P granules, which are associated with nuclear pore clusters on germ cell nuclei from mitosis to late pachytene stages of meiosis, but detach from nuclei during diakinesis as oocytes differentiate (Pitt et al., 2000; Strome and Wood, 1982). Transgenic worm strains were constructed expressing the P-granule component PGL-1 fused to either GFP or mRFP1. The tagged proteins localized correctly to nuclear-associated P granules, and to the detached cytoplasmic P granules (Fig. 1D, arrow and arrowhead, respectively). In addition, we found that the tagged proteins were present in much smaller cytoplasmic particles throughout the gonad (Fig. 1E,F, green square and yellow triangle; average diameter of cytoplasmic particles was 0.29±0.06 μm, n=86 particles). We observed similar small particles after immunostaining wild-type gonads for PGL-1, and found that additional P-granule components called GLH-1 and GLH-2 colocalized to the same particles (data not shown) (Gruidl et al., 1996; Roussell and Bennett, 1993). These small particles could arise from fragments of nuclear-associated P granules, or form de novo in the cytoplasm. In 18 out of 21 time-lapse movies, the small PGL-1::GFP or PGL-1::mRFP particles moved proximally along the core (Fig. 1D-G and H-L, arrowhead; see Movie 1 in the supplementary material). In the loop region, we observed several examples of fluorescently labeled P granules that moved proximally in the core after detaching from nuclei; some of these P granules were eventually incorporated into oocytes several cells distant from the oocyte nucleus of origin (see Movie 2-2 in the supplementary material).

We observed similar movement rates in pairwise recordings of DIC particles, mitochondria and PGL-1::GFP particles within the same gonads (data not shown), suggesting that there was a general streaming of core cytoplasm. We thus asked whether presumably inert materials could be transported by this flow. Fluorescently labeled polystyrene microspheres or small droplets of mineral oil (Table 2; Fig. 2; see Movies 2-1 and 2-2 in the supplementary material) were injected into gonads. Microspheres and oil droplets appeared to move at the same rate, and in the same pattern, as cytoplasmic P granules and DIC particles, respectively. We conclude that there is a general flow of core cytoplasm towards the proximal end of the gonad where oocytes enlarge, and refer to this flow as proximal streaming. Based on the average speed of DIC particles, we calculate that the flux in the core is about 270 μm^3/minute at 22°C. We estimate that oocytes increase in volume about 2.4-fold from influx of cytoplasm, and that roughly 30-40% of the final egg volume originates from cytoplasmic streaming (see calculations in Materials and methods).

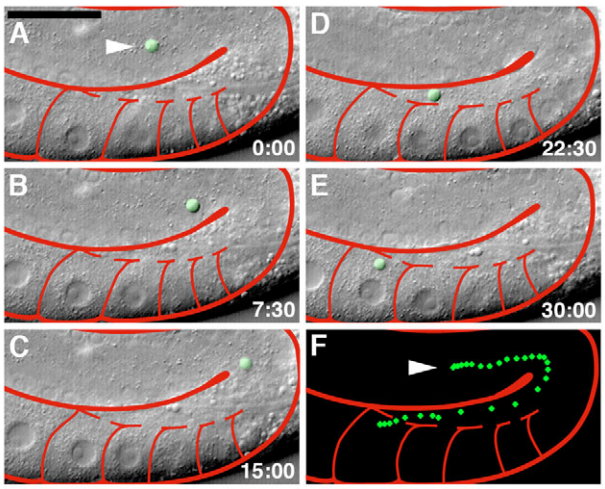

Fig. 2. Injected oil droplets are transported by cytoplasmic streaming in *C. elegans*. (**A-E**) Time-lapse images showing movement of an oil droplet (false green color, white arrowhead) over 30 minutes. (**F**) Position of the oil droplet in 1-minute intervals. Images are from Movie 2-1 in the supplementary material. Scale bar: 30 μm.

Table 2. Particle speeds in different mutant backgrounds and under the experimental conditions indicated

Strain/experiment	Particles	Temp.	Speed¶¶	*n****
Wild-type young adults*	DIC particles	25°C	7.8±2.4	6; 21
	DIC particles	22°C	6.0±2.1	3; 29
	Oil drop injection††	25°C	3.9±1.0	3; 3
	DIC particles after oil drop injection††	25°C	4.2±1.1	3; 50
	Microspheres‡‡	ND§§	4.8±1.0	2; 13
	PGL-1::GFP particles‡‡	ND§§	4.3±1.1	2; 15
Wild-type before first ovulation†	DIC particles	22°C	3.7±1.3	3; 33
Extruded gonads in EGTA*	DIC particles	22°C	5.0±2.7	7; 47
Old wild-type adults‡	DIC particles	22°C	0.0±0.3	3; 21
	PGL-1::GFP particles	ND§§	0.2±0.2	2; 15
Old wild-type after mating‡,¶	DIC particles	22°C	5.3±1.9	5; 43
fem-1(hc-17ts) young†	DIC particles	22°C	4.1±2.0	4; 38
fem-1(hc-17ts) old§	DIC particles	22°C	–0.2±0.6	3; 16
fem-3(q20gf)	DIC particles	22°C	5.2±1.5	5; 30
fog-1(q241) XO	DIC particles	22°C	2.5±0.8	4; 45
rme-2(b1008)	DIC particles	22°C	4.8±1.5	4; 30
*ced-3(n717); ced-1(e1735)***	DIC particles	22°C	4.2±1.8	6; 36
tba-2 RNAi	DIC particles	20°C	7.2±1.7	6; 45
Control RNAi	DIC particles	20°C	8.1±3.0	2; 12

Age of worms (days after last molt): *0.5-1 days; †very young worms right at or after molt; ‡5 days; §2-4 days.
¶Worms analyzed 4.8±2.3 hours after mating to wild-type males.
***ced-1* mutation used to confirm *ced-3* phenotype.
Speeds of two types of particles were measured in the same worms: ††after injection of a small oil drop and ‡‡after injection of fluorescent microspheres.
§§In confocal experiments, the temperature was within a range of 15-25°C.
¶¶Average speed in μm/minute±s.d.
***Number of worms analyzed; total number of particles analyzed.

Proximal streaming is dependent on oogenesis

In each of the above experiments, proximal streaming was observed in young adult hermaphrodite gonads with germ cells undergoing oogenesis. By contrast, we did not observe streaming in male gonads or in larval hermaphrodite gonads that lack oocytes (data not shown). Moreover, we found that streaming was not detectable in three types of animals that have extremely low rates of oocyte production: (1) young adult wild-type hermaphrodites after transfer to plates lacking food (data not shown); (2) old adult *fem-1(hc17ts)* 'feminized' hermaphrodites (Table 2); and (3) old adult wild-type hermaphrodites (Table 2) (Schisa et al., 2001). Streaming, and oocyte production, resumed in old wild-type hermaphrodites after mating to males (Table 2). We considered the possibility that ovulation itself might contribute to proximal streaming. Approximately every 23 minutes, contractions of somatic sheath cells that surround the proximal end of a gonad arm force the terminal, mature oocyte into the spermatheca (Hall et al., 1999; McCarter et al., 1999). *C. elegans* has a high internal hydrostatic pressure that maintains body shape, and this pressure might force core cytoplasm proximally into the space vacated by the oocyte. Although we observed a rapid and local redistribution of gonad cytoplasm coincident with each ovulation (see Movie 1 in the supplementary material), these discrete events appeared to be superimposed on otherwise continuous proximal streaming. Indeed, we observed proximal streaming under conditions in which ovulation does not occur: (1) very young adult wild-type hermaphrodites before the first ovulation; (2) *fem-3(q20gf)* mutant worms in which abnormal spermatogenesis prevents ovulation (Barton et al., 1987); and (3) *fog-1(q241)* 'males' (Table 2; for *fog-1*, see also below). We conclude that proximal streaming is associated with oogenesis, but is not caused by ovulation.

Although endocytosis of yolk lipoproteins does not account for most of the size increase of enlarging oocytes (see Introduction), we considered the possibility that yolk uptake might trigger streaming of other cytoplasmic materials; the yolk receptor RME-2 is expressed throughout the loop region of the gonad where oocytes enlarge (Grant and Hirsh, 1999). However, we observed that a GFP fusion of the yolk protein VIT-2 (Grant and Hirsh, 1999) begins to enter oocytes right after they have ceased receiving cytoplasm (data not shown). In addition, proximal streaming appears normal in the gonads of *rme-2(b1008)* mutants lacking the receptor (Table 2) (Grant and Hirsh, 1999). Finally, we asked if germline apoptosis is required for streaming. *ced-3(n717); ced-1(e1735)* double mutants lacking apoptosis showed normal streaming, although at a slightly reduced average particle speed compared with wild-type worms (Table 2) (Gumienny et al., 1999).

Proximal streaming does not require sheath cell contraction

Because the gonad sheath cells undergo frequent small contractions between ovulation events (McCarter et al., 1999), we considered the possibility that peristaltic waves of sheath contractions might contribute to proximal streaming. Contractions of wild-type sheath cells can be reduced or eliminated by depleting calcium with EGTA (Yin et al., 2004). We found that extruded gonads treated with 2 mM EGTA had few or no sheath contractions, but most appeared to have normal proximal streaming for at least 30 minutes (50 out of 53 gonads; Fig. 4E,F; Table 2; see Movie 4-3 in the supplementary material). Previous studies have shown that sheath contractions are highly reduced in feminized mutants such as *fem-1* (McCarter et al., 1999). Although we found that sheath cell contractions were often not detectable in time-lapse recordings of *fem-1(hc17)* young adults, these animals showed normal proximal streaming (Table 2). We next examined *fog-1(q241)* mutant 'males' that produce oocytes, but lack sheath cells and other female somatic gonad structures (Barton and Kimble, 1990; Jin et al., 2001). Gonad morphology in these mutants was highly aberrant and oogenesis very slow. Many animals showed very slow, or no, streaming. However, 7 of the 21 animals examined

showed streaming, at a reduced average speed of 2.5±0.8 μm/minute, into individual oocytes (Table 2). Taken together, these results suggest that sheath contractions are not essential for streaming, and that at least some streaming can occur in the absence of sheath cells.

Proximal streaming requires actomyosin but not microtubules

Because particle transport in animal and plant cells often requires microtubules and/or actomyosin, we asked whether either system was required for proximal streaming in the *C. elegans* gonad. Standard fixation and immunostaining procedures show only short, apparently random microtubules around *C. elegans* germ nuclei (Pitt et al., 2000). We developed a protocol that better preserves long microtubules (see Materials and methods). In the distal mitotic zone of the gonad, microtubules are present in the spindles of dividing cells or in apparently random interphase arrays (data not shown). Beginning with the pachytene zone, each germ nucleus is surrounded by a basket of microtubules that extend through the ring channel into the core of the gonad, and then continue proximally for long distances (Fig. 3A,B). Similar microtubules run through the ring channels of enlarging oocytes, bridging each oocyte with the core until cellularization (Fig. 3C). To investigate whether microtubules were required for proximal streaming, we depleted alpha- or beta-tubulin by dsRNA-mediated interference (RNAi). RNAi against single isoforms can result in depletion of multiple alpha- or beta-tubulin isoforms (Sonneville and Gonczy, 2004; Wright and Hunter, 2003). We found that dsRNA corresponding to *tba-2* (alpha-tubulin) and/or *tbb-1* and *tbb-2* (beta-tubulin) genes caused a marked depletion in microtubules detectable by immunostaining. For example, worms exposed to *tba-2* dsRNA for 24 hours had only short microtubules associated with the pachytene nuclei, and essentially no microtubules in the gonad core or in oocytes (Fig. 3, compare E with F). The treated animals produced only inviable embryos with severe cellular abnormalities (data not shown), and had variable but mild defects in gonad morphology. Nevertheless, proximal streaming appeared normal in the microtubule-depleted gonads (Fig. 3G,H; Table 2). After treatment with *tba-2* dsRNA for 48 hours, the gonads showed more pronounced morphological defects; germ nuclei were present in the normally anucleate gonad core, and many oocytes had abnormal shapes and sizes. However, most of these gonads continued to show proximal streaming. Remarkably, germ nuclei that were present inappropriately in the core also travelled proximally (see Movie 3-1 in the supplementary material). In a parallel series of experiments, we were unable to prevent streaming by depleting the gene products of 23 predicted microtubule motors and other microtubule-associated proteins (MAPs) by RNAi (see Materials and methods; data not shown). Depletion of some gene products, such as the dynein proteins DHC-1 and DLC-1 and the MAP DNC-1, resulted in gross morphological defects in the gonad. However, we observed proximal streaming in most of the treated animals (see Movie 3-2 in the supplementary material). Together, our results argue that microtubules are not essential for proximal streaming.

Previous studies have shown that actin and non-muscle myosin are highly enriched in the cortex of germ cells and oocytes (Maddox et al., 2005; Strome, 1986), but have not described localization throughout the cytoplasm. We used two staining procedures to visualize actin with fluorescent phalloidin (see Materials and methods). Using method I, stained filaments were significantly enriched around oocyte nuclei, with relatively few filaments visible in the core region of most gonads (Fig. 4A). A small fraction of these gonads showed fine filaments aligned in the direction of streaming in the core and ring channels, and this appearance was observed consistently using fixation method II (Fig. 4B; see Movies 4-1 and 4-2 in the supplementary material). With method II, most of the filaments within oocytes appeared to be randomly oriented, except for groups of filaments that extended between the oocyte nucleus and the plasma membrane. By contrast, numerous filaments in the ring channels of enlarging oocytes were oriented in the direction of streaming. Many of these filaments appeared to extend from the core plasma membrane toward and into enlarging oocytes (Fig. 4B, arrowheads). The staining intensity of these oriented filaments was comparable to that of the apparently randomly oriented filaments in the core region of the pachytene area (Fig. 4C).

To determine whether microfilaments are required for proximal streaming, we analyzed gonads extruded in culture medium with or without inhibitors of actin polymerization or myosin light chain kinase; EGTA was added to the medium in all experiments to prevent sheath cell contractions. In gonads treated with the actin depolymerizing drug latrunculin A (LatA) (Severson and Bowerman, 2003; Spector et al., 1983) at 0.5-5 μM, the actin-rich

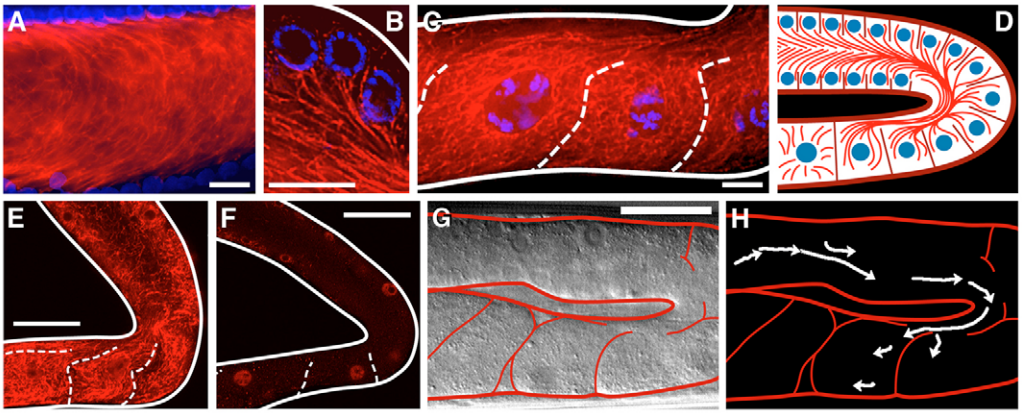

Fig. 3. Gonad microtubules are not required for proximal streaming in *C. elegans*. (**A**) Microtubules (red) and nuclei (blue) in pachytene region. Proximal is to the right. (**B**) High magnification image of microtubules around individual germ nuclei. (**C**) Microtubules extending between enlarging oocytes and gonad core. Oocyte membranes are indicated by dashed lines. (**D**) Summary diagram of gonad microtubules. (**E**,**F**) Gonads immunostained for α-tubulin after treating worms with empty-vector control (E) or an α-tubulin RNAi feeding strain (F) for 24 hours. (**G**,**H**) Normal particle movement in an α-tubulin RNAi-treated gonad; 2-minute particle tracks. Scale bars: 10 μm in A-C; 30 μm in E-G.

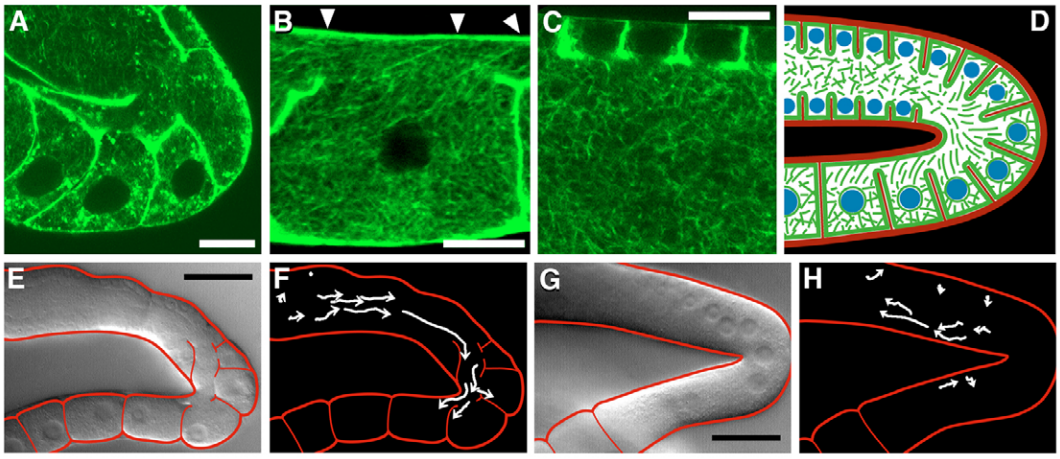

Fig. 4. The actomyosin cytoskeleton is required for streaming in *C. elegans*. (**A-C**) Phalloidin-stained microfilaments (green). (A) Low magnification view of enlarging oocytes in loop; fixation method I. (B) High magnification view of enlarging oocyte; fixation method II. Note the long filaments (arrowheads) extending from the core plasma membrane into the oocyte. (C) Pachytene region. (**D**) Summary diagram of gonad microfilaments. (**E**,**F**) Cytoplasmic streaming in gonad extruded in culture medium with EGTA; 2-minute particle tracks. (**G**,**H**) Abnormal, reversed streaming in gonad extruded in culture medium with latrunculin A and EGTA; 2-minute particle tracks. Scale bars: 10 μm in A-C; 30 μm in E,G.

lateral membranes of germ cells and enlarging oocytes appeared to collapse. Although a few gonads treated with LatA showed normal proximal streaming (2 of 13), most lacked streaming (9 of 13) or had aberrant, reverse flow in the distal direction (2 of 13; Fig. 4G,H); 50 of 53 control gonads without LatA treatment showed normal proximal streaming (Fig. 4E,F; see Movie 4-3 in the supplementary material).

Extruded gonads treated with lowered levels of LatA showed reduced, or no, membrane defects, but continued to show streaming defects: 6 of 19 gonads exposed to 0.25-0.4 μM LatA lacked streaming or had aberrant, reverse flow in the distal direction (data not shown). These results suggest that the role of actin in streaming is at least partially separate from its role in plasma membrane integrity.

Extruded gonads treated with the myosin light chain kinase inhibitor ML-7 (Lee and Goldstein, 2003; Saitoh et al., 1987) at 250 μM showed proximal streaming defects and membrane defects similar to those induced by 0.5-5 μM LatA. The treated gonads either lacked proximal streaming (4 of 8), showed only brief streaming (1 of 8), or had aberrant flow in the distal direction (3 of 8). Gonads treated with 60 μM ML-7 usually showed normal proximal streaming for several minutes, but then stopped streaming either just before, or coincident with, a collapse in plasma membrane structure (3 of 9 and 6 of 9 gonads, respectively). Finally, we observed rare cases of reversed streaming in gonads that appeared to have intact plasma membranes (see Movie 4-4 in the supplementary material). Together, these results indicate that proximal streaming requires the actomyosin cytoskeleton.

Streaming forces are generated in or near oocytes

To determine where the forces involved in streaming are generated, we attempted to block the gonad core at different positions along the distal-proximal axis by injecting large drops of mineral oil into the gonads of intact worms. We found that cytoplasmic particles were unable to travel through or around oil drops injected into the core, indicating that the gonad was effectively partitioned into separate zones. Blocking the core within the pachytene region had no apparent effect on proximal streaming (n=2; Fig. 5A-C). We next injected oil drops between the pachytene region and the loop. In the pachytene region, particles either did not move or moved slowly in a reversed, distal direction (Fig. 5D-F; see Movie 5-1 in the supplementary material). Surprisingly, proximal streaming appeared relatively normal in the loop and enlarging oocytes, despite the fact that only a small segment of gonad core separated the oil drop from the enlarging oocytes. Moreover, several of these truncated proximal gonads showed abnormal patterns of flow between adjacent oocytes: large proximal oocytes continued to expand, apparently by pulling cytoplasm from neighboring smaller oocytes that simultaneously decreased in size (see Movie 5-1 in the supplementary material). When we blocked all enlarging oocytes with a large drop of oil, streaming in the gonad ceased entirely (n=6; see Movie 5-2 in the supplementary material). Finally, injecting oil into already cellularized oocytes did not affect streaming (n=3). Together, these results suggest that proximal streaming is caused by forces generated within or near the enlarging oocytes, rather than in the pachytene area.

If the oocytes indeed generated their own streaming force, damage of individual oocytes might prevent influx of cytoplasm. Conversely, if cytoplasm was pushed, rather than pulled, through the ring channel into an enlarging oocyte, damaged oocytes might remain competent to receive streaming cytoplasm. We attempted to mechanically damage individual enlarging oocytes by penetrating their apical cell membrane with a microneedle, and marking the damaged cells with a small oil droplet (Fig. 5G-I; see Movie 5-3 in the supplementary material). In almost all cases (6 of 7), cytoplasm immediately ceased streaming into the injected oocyte. In 2 of 7 cases, cytoplasm and the small oil droplet flowed out of the damaged oocyte and into neighboring oocytes on both sides (Fig. 5G-I; see Movie 5-3 in the supplementary material). Cytoplasm flowing from a damaged oocyte into the distal neighbor moved opposite to the general, proximal direction of cytoplasmic streaming, supporting the model that forces in or around individual oocytes generate flow.

DISCUSSION

In this report we have demonstrated that cytoplasmic streaming occurs in the core of the *C. elegans* gonad. We have shown directly that streaming transports mitochondria and the germline-specific protein PGL-1 within the core. Because streaming can also transport

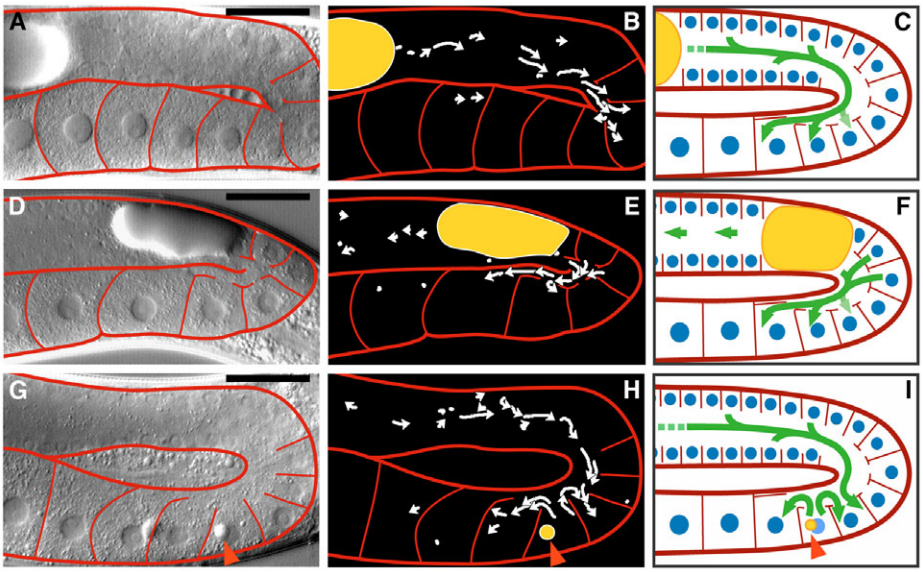

Fig. 5. The force driving proximal streaming appears to be generated close to or within the enlarging oocytes. Drops of mineral oil (yellow) were injected into different areas of the *C. elegans* gonad. (**A**,**D**,**G**) DIC image. (**B**,**E**,**H**) 2-minute particle tracks. (**C**,**F**,**I**) summary diagrams. (A-C) Blocking the early pachytene area results in normal proximal streaming. (D-F) Particle movement after injection of an oil drop between the late pachytene area and loop. (G-I) An oocyte was damaged by injecting a small mineral oil droplet directly into it (red arrowhead). Scale bars: 30 μm.

polystyrene beads, small oil droplets and nuclei that are mislocalized to the core, we argue that streaming is a general process involving most cytoplasmic materials. Streaming transfers material from a region of transcriptionally active pachytene-stage nuclei in the distal gonad into the proximal region of enlarging, transcriptionally quiescent oocytes. These results provide a mechanistic explanation for previous observations on the distribution of RNA in the gonad. Labeled-uridine incorporation showed that nascent RNA (largely rRNA) first appears in pachytene nuclei, and subsequently accumulates in the gonad core before appearing in oocyte cytoplasm (Gibert et al., 1984; Schisa et al., 2001; Starck, 1977). Because materials are transported from numerous pachytene-stage nuclei into single, enlarging oocytes, the pachytene-stage nuclei can be considered a nurse cell population. Thus, *C. elegans* appears to use a strategy in which hundreds of syncytial germ cells contribute materials to an oocyte, in contrast to the 15 highly polyploid nurse cells in *Drosophila* (Cooley and Theurkauf, 1994).

Several lines of evidence suggest that the forces that move cytoplasm proximally along the core are generated either in, or very close to, the enlarging oocytes. First, we have shown that contractions of the somatic sheath cells of the gonad are not essential for streaming. Mutants lacking the sheath cells often showed abnormally slow streaming, suggesting that these cells might directly or indirectly influence flow rates. However, the fact that flow can occur in such gonads suggests that the sheath cells do not generate the streaming forces. Second, our oil-drop experiments show that partitioning the gonad between the pachytene area and loop does not inhibit streaming into oocytes. Third, core cytoplasm does not stream into an oocyte that is damaged mechanically. This latter result argues that cytoplasm is not forced into an oocyte, and suggests a model in which cytoplasm is pulled into oocytes. This model contrasts with results in *Drosophila* indicating that nurse cell contraction pushes cytoplasm into the oocyte (Cooley and Theurkauf, 1994; Mahajan-Miklos and Cooley, 1994).

Cytoplasmic streaming and the cytoskeleton

The rate of cytoplasmic streaming in *C. elegans* gonads is comparable to the microtubule-dependent 'fast' streaming that occurs in *Drosophila* oocytes prior to the dumping of nurse cell contents (Serbus et al., 2005). Although gonads contain large numbers of long microtubules that are oriented in the direction of streaming, our RNAi studies suggest that microtubules do not play a major role in proximal streaming. These results do not exclude the possibility of a minor role in organelle transport. For example, plant cells that undergo rapid actomyosin-based streaming of their bulk cytoplasm can have much slower kinesin- and microtubule-based transport of specific organelles (Shimmen and Yokota, 2004). One interesting possibility is that microtubules in *C. elegans* function in moving materials radially, away from the pachytene nuclei and towards the midline of the gonad core. Previous studies have shown that RNA accumulates along the midline of the core in old adults (Schisa et al., 2001), and we have shown here that old adults lack proximal streaming.

Whereas microtubule depletion did not cause major defects in proximal streaming, we observed a lack of streaming or aberrant, reverse streaming when gonads were treated with inhibitors of the actomyosin cytoskeleton. We do not yet understand the basis for the reversed flow, and it is possible that this flow has no mechanistic relationship to normal streaming. For example, treated gonads might expand radially as the cytoskeleton breaks down. Gonads treated with high concentrations of actomyosin inhibitors showed a collapse of the lateral plasma membranes, similar to the regression of the contractile ring in dividing embryonic cells that are treated with microfilament inhibitors (Strome and Wood, 1983). When we used lower concentrations of actomyosin inhibitors, proximal streaming often terminated before any apparent collapse of the lateral membranes. This result suggests that proximal streaming involves an actin-mediated event that is at least partially separate from the role of actin in membrane integrity.

Enlarging oocytes are associated with diverse actin populations that might contribute to streaming forces. The cortex is highly enriched in actin, there is a meshwork of filaments throughout the oocyte, and filaments that are aligned in the direction of flow extend into the oocyte through the ring channels. Several models for actin-dependent streaming can be considered (Fig. 6A-D). Newly fertilized *C. elegans* embryos exhibit cytoplasmic streaming towards their posterior pole that is thought to be driven by a reciprocal contraction of cortical actin toward the anterior pole (Hird and White, 1993; Munro et al., 2004); a similar process could operate in

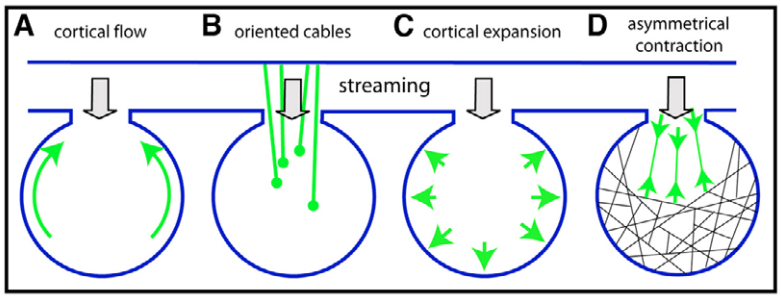

Fig. 6. Models for oocyte-driven actin-dependent proximal streaming in *C. elegans*. Gray arrows indicate direction of cytoplasmic streaming into enlarging oocytes (blue outline). (**A**) Cortical contraction (green arrows) generates reciprocal cytoplasmic flow. (**B**) Particle transport along oriented actin cables (green). (**C**) Expansion of cortical surface. (**D**) Contractile actomyosin network at the entrance to an oocyte linked to a stable interior meshwork.

enlarging oocytes (Fig. 6A). The rate of cytoplasmic streaming in the embryo is about 4-5 μm/min, comparable to the rate we observe for streaming into oocytes. However, because expanding oocytes are not closed systems like embryos, it is difficult to imagine how cortical contraction alone would result in influx of cytoplasm. In addition, we did not observe sustained movements of cortical granules, or asymmetries in the distribution of cortical actin.

In a variety of plant cells, streaming organelles are associated with myosins that allow them to slide along oriented actin cables; the cables can be composed of as many as 100 actin microfilaments of uniform polarity, bundled together by proteins such as villin and fimbrin (Huang et al., 2005; Nagai and Rebhun, 1966; Shimmen and Yokota, 2004). We have described actin-containing filaments that extend from the outer plasma membrane of the gonad core and into the enlarging oocytes. Thus, it is possible that these filaments have a common polarity, an important element of a cable model for streaming (Fig. 6B). Streaming rates can be 150 μm/min in *Arabidopsis* to approaching 600 μm/min in *Chara* (Holweg and Nick, 2004; Shimmen and Yokota, 2004). In yeast, *ASH1* mRNA and Kar9p are transported by myosins along actin cables from mother to daughter cells at rates of 30 μm/min and 90 μm/min, respectively (Beach et al., 2000; Bertrand et al., 1998). By comparison, the rate of streaming into *C. elegans* oocytes is relatively slow, at about only 8 μm/min.

The expansion of the plasma membrane of an enlarging oocyte is reminiscent of the expanding leading edges of motile cells (Fig. 6C). Leading edge extension is thought to be driven by the expansion of an underlying branched network of actin filaments dependent on the Arp2/3 complex (reviewed by Pollard and Borisy, 2003). Similarly, expansion of cellular lobes in *Arabidopsis* pavement cells is dependent on actin and regulators of the Arp2/3 complex (Fu et al., 2005). However, none of the known *C. elegans* Arp2/3 genes and regulators have been reported to be required for normal oocyte size or ovulation rate.

A striking feature of streaming in the *C. elegans* gonad is the relative absence of particle movement in the oocyte interior compared with particle movement through the gonad core and ring channels. Our attempts to fix actin filaments in the gonad suggest that filaments in the core and ring channels are much harder to preserve, and therefore possibly more dynamic, than actin in the oocyte interior. If a dynamic, contractile actomyosin network in the core and ring channels (Fig. 6D, green arrows) is linked mechanically to a relatively stable network within the oocyte (Fig. 6D, black lines), this asymmetry could pull particles into the oocyte. Analogous models of asymmetric actomyosin dynamics have been proposed for cytoplasmic streaming into the leading edges of amoeboid cells and for fountain streaming in the *Drosophila* syncytial blastoderm (Odell, 1977; von Dassow and Schubiger, 1994). In future studies, it should be possible to evaluate these and other models for streaming, as tools become available to visualize actomyosin dynamics within the gonad.

We thank Tim Schedl and Arne IJpma for experimental suggestions; Jeremy Nance, Rafal Ciosk, Edwin Munro and all members of the Priess laboratory for helpful discussions and critical reading of the manuscript; and Julio Vazquez and Dave McDonald for assistance with confocal imaging and movie files. U.W. was supported by a fellowship from the Center for Research in Reproduction and Contraception, University of Washington, Seattle, and the Howard Hughes Medical Institute. J.R.P. and E.A.J. are supported by the Howard Hughes Medical Institute.

Supplementary material

Supplementary material for this article is available at
http://dev.biologists.org/cgi/content/full/134/12/2227/DC1

References

Barton, M. K. and Kimble, J. (1990). fog-1, a regulatory gene required for specification of spermatogenesis in the germ line of Caenorhabditis elegans. *Genetics* **125**, 29-39.
Barton, M. K., Schedl, T. B. and Kimble, J. (1987). Gain-of-function mutations of fem-3, a sex-determination gene in Caenorhabditis elegans. *Genetics* **115**, 107-119.
Beach, D. L., Thibodeaux, J., Maddox, P., Yeh, E. and Bloom, K. (2000). The role of the proteins Kar9 and Myo2 in orienting the mitotic spindle of budding yeast. *Curr. Biol.* **10**, 1497-1506.
Bertrand, E., Chartrand, P., Schaefer, M., Shenoy, S. M., Singer, R. H. and Long, R. M. (1998). Localization of ASH1 mRNA particles in living yeast. *Mol. Cell* **2**, 437-445.
Bohrmann, J. and Biber, K. (1994). Cytoskeleton-dependent transport of cytoplasmic particles in previtellogenic to mid-vitellogenic ovarian follicles of Drosophila: time-lapse analysis using video-enhanced contrast microscopy. *J. Cell Sci.* **107**, 849-858.
Brenner, S. (1974). The genetics of Caenorhabditis elegans. *Genetics* **77**, 71-94.
Campbell, R. E., Tour, O., Palmer, A. E., Steinbach, P. A., Baird, G. S., Zacharias, D. A. and Tsien, R. Y. (2002). A monomeric red fluorescent protein. *Proc. Natl. Acad. Sci. USA* **99**, 7877-7882.
Cavaliere, V., Taddei, C. and Gargiulo, G. (1998). Apoptosis of nurse cells at the late stages of oogenesis of Drosophila melanogaster. *Dev. Genes Evol.* **208**, 106-112.
Cooley, L. and Theurkauf, W. E. (1994). Cytoskeletal functions during Drosophila oogenesis. *Science* **266**, 590-596.
Fire, A., Xu, S., Montgomery, M. K., Kostas, S. A., Driver, S. E. and Mello, C. C. (1998). Potent and specific genetic interference by double-stranded RNA in Caenorhabditis elegans. *Nature* **391**, 806-811.
Foe, V. E. and Alberts, B. M. (1983). Studies of nuclear and cytoplasmic behaviour during the five mitotic cycles that precede gastrulation in Drosophila embryogenesis. *J. Cell Sci.* **61**, 31-70.
Fu, Y., Gu, Y., Zheng, Z., Wasteneys, G. and Yang, Z. (2005). Arabidopsis interdigitating cell growth requires two antagonistic pathways with opposing action on cell morphogenesis. *Cell* **120**, 687-700.
Gibert, M. A., Starck, J. and Beguet, B. (1984). Role of the gonad cytoplasmic core during oogenesis of the nematode Caenorhabditis elegans. *Biol. Cell* **50**, 77-85.
Grant, B. and Hirsh, D. (1999). Receptor-mediated endocytosis in the Caenorhabditis elegans oocyte. *Mol. Biol. Cell* **10**, 4311-4326.
Greenstein, D. (2005). Control of oocyte meiotic maturation and fertilization. In *WormBook* (ed. The *C. elegans* Research Community), WormBook, doi/10.1895/wormbook.1.53.1, http://www.wormbook.org.
Gruidl, M. E., Smith, P. A., Kuznicki, K. A., McCrone, J. S., Kirchner, J., Roussell, D. L., Strome, S. and Bennett, K. L. (1996). Multiple potential germ-line helicases are components of the germ-line-specific P granules of Caenorhabditis elegans. *Proc. Natl. Acad. Sci. USA* **93**, 13837-13842.
Gumienny, T. L., Lambie, E., Hartwieg, E., Horvitz, H. R. and Hengartner, M. O. (1999). Genetic control of programmed cell death in the Caenorhabditis elegans hermaphrodite germline. *Development* **126**, 1011-1022.
Hall, D. H., Winfrey, V. P., Blaeuer, G., Hoffman, L. H., Furuta, T., Rose, K. L.,

Hobert, O. and Greenstein, D. (1999). Ultrastructural features of the adult hermaphrodite gonad of Caenorhabditis elegans: relations between the germ line and soma. *Dev. Biol.* **212**, 101-123.
Hird, S. N. and White, J. G. (1993). Cortical and cytoplasmic flow polarity in early embryonic cells of Caenorhabditis elegans. *J. Cell Biol.* **121**, 1343-1355.
Hirsh, D., Oppenheim, D. and Klass, M. (1976). Development of the reproductive system of Caenorhabditis elegans. *Dev. Biol.* **49**, 200-219.
Holweg, C. and Nick, P. (2004). Arabidopsis myosin XI mutant is defective in organelle movement and polar auxin transport. *Proc. Natl. Acad. Sci. USA* **101**, 10488-10493.
Huang, S., Robinson, R. C., Gao, L. Y., Matsumoto, T., Brunet, A., Blanchoin, L. and Staiger, C. J. (2005). Arabidopsis VILLIN1 generates actin filament cables that are resistant to depolymerization. *Plant Cell* **17**, 486-501.
Jin, S. W., Kimble, J. and Ellis, R. E. (2001). Regulation of cell fate in Caenorhabditis elegans by a novel cytoplasmic polyadenylation element binding protein. *Dev. Biol.* **229**, 537-553.
Kamath, R. S. and Ahringer, J. (2003). Genome-wide RNAi screening in Caenorhabditis elegans. *Methods* **30**, 313-321.
Kimble, J. and Sharrock, W. J. (1983). Tissue-specific synthesis of yolk proteins in Caenorhabditis elegans. *Dev. Biol.* **96**, 189-196.
Korchak, H. M., Rich, A. M., Wilkenfeld, C., Rutherford, L. E. and Weissmann, G. (1982). A carbocyanine dye, DiOC6(3), acts as a mitochondrial probe in human neutrophils. *Biochem. Biophys. Res. Commun.* **108**, 1495-1501.
Lee, J. Y. and Goldstein, B. (2003). Mechanisms of cell positioning during C. elegans gastrulation. *Development* **130**, 307-320.
Maddox, A. S., Habermann, B., Desai, A. and Oegema, K. (2005). Distinct roles for two C. elegans anillins in the gonad and early embryo. *Development* **132**, 2837-2848.
Mahajan-Miklos, S. and Cooley, L. (1994). Intercellular cytoplasm transport during Drosophila oogenesis. *Dev. Biol.* **165**, 336-351.
McCarter, J., Bartlett, B., Dang, T. and Schedl, T. (1999). On the control of oocyte meiotic maturation and ovulation in Caenorhabditis elegans. *Dev. Biol.* **205**, 111-128.
Mello, C. C., Kramer, J. M., Stinchcomb, D. and Ambros, V. (1991). Efficient gene transfer in C. elegans: extrachromosomal maintenance and integration of transforming sequences. *EMBO J.* **10**, 3959-3970.
Motegi, F., Velarde, N. V., Piano, F. and Sugimoto, A. (2006). Two phases of astral microtubule activity during cytokinesis in C. elegans embryos. *Dev. Cell* **10**, 509-520.
Munro, E., Nance, J. and Priess, J. R. (2004). Cortical flows powered by asymmetrical contraction transport PAR proteins to establish and maintain anterior-posterior polarity in the early C. elegans embryo. *Dev. Cell* **7**, 413-424.
Nagai, R. and Rebhun, L. I. (1966). Cytoplasmic microfilaments in streaming Nitella cells. *J. Ultrastruct. Res.* **14**, 571-589.
Nance, J., Munro, E. M. and Priess, J. R. (2003). C. elegans PAR-3 and PAR-6 are required for apicobasal asymmetries associated with cell adhesion and gastrulation. *Development* **130**, 5339-5350.
Odell, G. M. (1977). A continuum theory of Allen's frontal contraction model of amoeboid pseudopodium extension. *J. Mechanochem. Cell Motil.* **4**, 1-13.
Park, F. D. and Priess, J. R. (2003). Establishment of POP-1 asymmetry in early C. elegans embryos. *Development* **130**, 3547-3556.
Pepling, M. E., de Cuevas, M. and Spradling, A. C. (1999). Germline cysts: a conserved phase of germ cell development? *Trends Cell Biol.* **9**, 257-262.
Pitt, J. N., Schisa, J. A. and Priess, J. R. (2000). P granules in the germ cells of Caenorhabditis elegans adults are associated with clusters of nuclear pores and contain RNA. *Dev. Biol.* **219**, 315-333.
Pollard, T. D. and Borisy, G. G. (2003). Cellular motility driven by assembly and disassembly of actin filaments. *Cell* **112**, 453-465.
Praitis, V., Casey, E., Collar, D. and Austin, J. (2001). Creation of low-copy integrated transgenic lines in Caenorhabditis elegans. *Genetics* **157**, 1217-1226.
Robinson, D. N. and Cooley, L. (1997). Genetic analysis of the actin cytoskeleton in the Drosophila ovary. *Annu. Rev. Cell Dev. Biol.* **13**, 147-170.
Roussell, D. L. and Bennett, K. L. (1993). glh-1, a germ-line putative RNA helicase from Caenorhabditis, has four zinc fingers. *Proc. Natl. Acad. Sci. USA* **90**, 9300-9304.
Saitoh, M., Ishikawa, T., Matsushima, S., Naka, M. and Hidaka, H. (1987). Selective inhibition of catalytic activity of smooth muscle myosin light chain kinase. *J. Biol. Chem.* **262**, 7796-7801.
Schedl, T. (1997). Developmental genetics of the germ line. *In C. elegans* II (ed. D. Riddle, T. Blumenthal, B. Meyer and J. Priess), pp. 241-270. Cold Spring Harbor: Cold Spring Harbor Laboratory Press.
Schisa, J. A., Pitt, J. N. and Priess, J. R. (2001). Analysis of RNA associated with P granules in germ cells of C. elegans adults. *Development* **128**, 1287-1298.
Serbus, L. R., Cha, B. J., Theurkauf, W. E. and Saxton, W. M. (2005). Dynein and the actin cytoskeleton control kinesin-driven cytoplasmic streaming in Drosophila oocytes. *Development* **132**, 3743-3752.
Severson, A. F. and Bowerman, B. (2003). Myosin and the PAR proteins polarize microfilament-dependent forces that shape and position mitotic spindles in Caenorhabditis elegans. *J. Cell Biol.* **161**, 21-26.
Shimmen, T. and Yokota, E. (2004). Cytoplasmic streaming in plants. *Curr. Opin. Cell Biol.* **16**, 68-72.
Sonneville, R. and Gonczy, P. (2004). Zyg-11 and cul-2 regulate progression through meiosis II and polarity establishment in C. elegans. *Development* **131**, 3527-3543.
Spector, I., Shochet, N. R., Kashman, Y. and Groweiss, A. (1983). Latrunculins: novel marine toxins that disrupt microfilament organization in cultured cells. *Science* **219**, 493-495.
Starck, J. (1977). Radioautographic study of RNA synthesis in Caenorhabditis elegans (Bergerac Variety) oogenesis. *Biol. Cell* **30**, 181-182.
Strome, S. (1986). Fluorescence visualization of the distribution of microfilaments in gonads and early embryos of the nematode Caenorhabditis elegans. *J. Cell Biol.* **103**, 2241-2252.
Strome, S. and Wood, W. B. (1982). Immunofluorescence visualization of germ-line-specific cytoplasmic granules in embryos, larvae, and adults of Caenorhabditis elegans. *Proc. Natl. Acad. Sci. USA* **79**, 1558-1562.
Strome, S. and Wood, W. B. (1983). Generation of asymmetry and segregation of germ-line granules in early C. elegans embryos. *Cell* **35**, 15-25.
Theurkauf, W. E. and Hazelrigg, T. I. (1998). In vivo analyses of cytoplasmic transport and cytoskeletal organization during Drosophila oogenesis: characterization of a multi-step anterior localization pathway. *Development* **125**, 3655-3666.
Theurkauf, W. E., Smiley, S., Wong, M. L. and Alberts, B. M. (1992). Reorganization of the cytoskeleton during Drosophila oogenesis: implications for axis specification and intercellular transport. *Development* **115**, 923-936.
Thomas, C., DeVries, P., Hardin, J. and White, J. (1996). Four-dimensional imaging: computer visualization of 3D movements in living specimens. *Science* **273**, 603-607.
Valle, D. (1993). Vitellogenesis in insects and other groups – a review. *Mem. Inst. Oswaldo Cruz* **88**, 1-26.
von Dassow, G. and Schubiger, G. (1994). How an actin network might cause fountain streaming and nuclear migration in the syncytial Drosophila embryo. *J. Cell Biol.* **127**, 1637-1653.
Wright, A. J. and Hunter, C. P. (2003). Mutations in a beta-tubulin disrupt spindle orientation and microtubule dynamics in the early Caenorhabditis elegans embryo. *Mol. Biol. Cell* **14**, 4512-4525.
Yin, X., Gower, N. J., Baylis, H. A. and Strange, K. (2004). Inositol 1,4,5-trisphosphate signaling regulates rhythmic contractile activity of myoepithelial sheath cells in Caenorhabditis elegans. *Mol. Biol. Cell* **15**, 3938-3949.